INFLUENCE OF THE BACKING AND COVERING LAYERS THICKNESSES IN THE STRESS FIELDS IN AUTOMOTIVE JOURNAL BEARINGS

Felipe José Passos Silva
Unesp – Faculdade de Engenharia de Guaratinguetá – Departamento de Mecânica
felipejpsilva@yahoo.com.br

Fernando de Azevedo Silva
Unesp – Faculdade de Engenharia de Guaratinguetá – Departamento de Mecânica
fazevedo@feg.unesp.br

Abstract. *This work aims at to study the influence of the backing and covering layers thicknesses in the stress fields in automotive journal bearings submitted to hydrodynamic stress distribution. For this, software ANSYS® will be used basing on finite elements method. Thus, it's intended to evaluate the relation between the stress distributions caused by backing and covering layers thicknesses with fatigue failure, which is the most common type of failure that occurs in bearings. It is common to accept that the fatigue resistance of the bearing can be increased by reduction of the white metal thickness.*

Keywords: *Journal bearings, stress field, finite element method, thickness.*

1. Introduction

Journal bearings are simple geometry component and they are essential in automotive engines, because they are important always that it will have pieces in relative movement (figure 1). Journal bearings are generally used where a specific alignment should be kept between the pieces or where a force should be transmitted of a piece to another one. The bearings have a surface constituted by antifriction material, whose hardness and temperature of melting are lower than of the shaft material, ensuring, a grip and wear reduction of the more expensive and difficult substitution mobile pieces, such as the crankshaft. Thus, the bearings protect and extend the useful life of the most expensive and greater importance elements in the system.

Figure 1. Photo of the automotive journal bearing in study.

The most common antifriction material in automotive journal bearings is babbitt, that it is a white metal. White metal are chosen because they have low hardness and temperature of melting.

There are many factors and parameters that could cause bearing failure. These may occur in any stage of the designing, manufacturing and service conditions in a journal bearing. Generally, these bearing failure are related with stress sources.

There are many stress sources in bearings, as, for example, pressure gradient, flexibilities of backing and housing materials, presence of oil grooves, non-uniform housing supports and temperature distributions, surface roughness, backing layer thickness, covering layer thickness, assembly problems, among others (Hacifazlioglu and Karadeniz, 1996). One of the most common types of evidenced failures is the surface fatigue, which it appears in the form of surface cracks. Reverse stresses in the bearing layer can cause surface fatigue. These failures can be induced in the surface due to the direct floating stresses or in the bond surface due to the shear floating stresses.

The thickness and temperature effects in the alloys fatigue strength are similar. The fatigue strength reduces with the increase of the layer thickness and the temperature levels.

In accordance with Forrester and Chalmers (1945), it is common to accept that the fatigue resistance of the bearing can be increased by reduction of the white metal thickness. Therefore, it is important to evaluate the influence of the thickness in the bearing stress field.

2. Hydrodynamic pressure

In accordance with Norton (1998), the hydrodynamic pressure can be gotten through Ocvirk solution or short bearings solution, as shown to follow:

$$p = \frac{\eta U}{r c_r^{\,2}} \left[\frac{l^2}{4} - z^2 \right] \frac{3\varepsilon \operatorname{sen}\theta}{(1+\varepsilon\cos\theta)^3} \tag{1}$$

where:

η: absolute viscosity [mPa.s];

U: linear velocity [m/s];

r: journal radius [m];

c_r: radial clearance [m];

l: journal length [m];

z: escape direction (it is considered null for short bearings);

ε: excentricity ratio; and

θ: pressure angle [rad].

This solution is valid to $\theta = 0$ to π, with pressure assumed as zero in the other half of the circumference and also for *l/d* ratios between ¼ to 1, being *d* the journal diameter.

Pressure *p* varies nonlinear with θ and has its peak in the second quadrant. The value of $\theta_{máx}$, which is the angle where the pressure is maximum, can be found through the equation:

$$\theta_{máx} = \cos^{-1}\left[\frac{1-\sqrt{1+24\varepsilon^2}}{4\varepsilon} \right] \tag{2}$$

This angle is measured in the axis that varies along of the eccentricity line between the centers of the bearing and journal, to 0 to π. To locate the bearing positioning referring to the angle θ, exist an angle ϕ that is the angle between the force F (considered vertical) applied to the journal and $\theta = \pi$. This angle can be gotten through:

$$\phi = \tan^{-1}\left[\frac{\pi\sqrt{1-\varepsilon^2}}{4\varepsilon} \right] \tag{3}$$

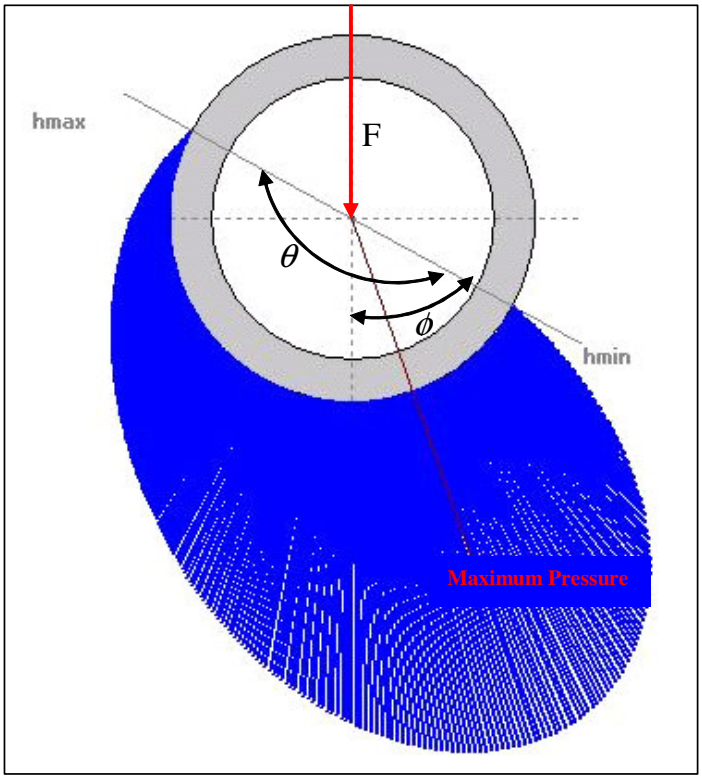

Figure 2. Scheme of bearing pressure profile detailing the θ and ϕ angles.

Table 1 shows referring data of the bearing functioning, to be able to get the hydrodynamic pressure profile.

Tabel 1. Data to get profile of the operating pressure in the bearing.

Velocity (n)	2500 [rpm] or 41.67 [rps]
Journal diameter (d)	42.38 [mm]
Bearing length (l)	17.94 [mm]
l/d ratio	0.4233
Operation temperature	95° C to 110° C
Lubricant	SAE 50
Absolute viscosity	12 [mPa.s]
Radial clearance (c_r)	3.2×10^{-5} [m]
Linear velocity (U)	5.55 [m/s]
Ocvirk number	45
Eccentricity ratio (e)	0.862708
Maximum pressure	35.76 [MPa]
θ_{max}	165.64°
ϕ	24.7°

Figure 3 shows the hydrodynamic pressure profile applied to the bearing. It is possible to note that the pressure acts in 180° of the bearing (114.7° to 294.7°). The others 180° are free of the hydrodynamic pressure actuation.

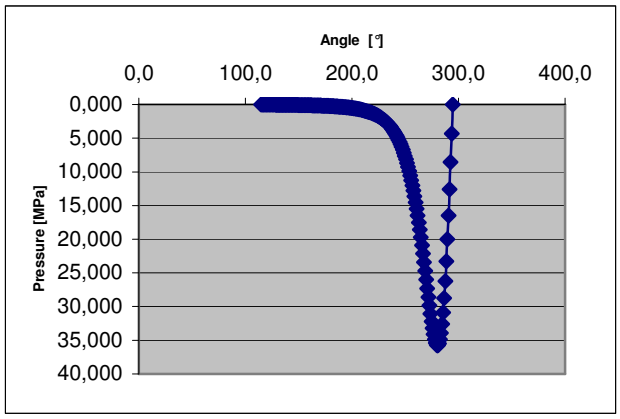

Figure 3. Applied hydrodynamic pressure profile.

3. Simulation

This study consists in the analysis of the effect of backing and covering (babbitt) thicknesses in the bearing. In the analysis, the bearing models were developed in the bidimensional plan, inside of the elastic regime and it was assumed that deformation along the bearing longitudinal axis (coordinate axis *z*) doesn't occur. This situation characterizes the plain state of deformation. For this, first the bearing with its real measures was simulated in software ANSYS®. Later, four models had been made, two models with variations in the covering thickness, and others two models with variations in the backing thickness. Table 2 shows the measures of each model.

Table 2. Dimensions of each model.

Model	Journal diameter	Covering thickness	Backing thickness
1 (real)	42.38 [mm]	0.35 [mm]	1.11 [mm]
2	42.38 [mm]	0.20 [mm]	1.11 [mm]
3	42.38 [mm]	0.50 [mm]	1.11 [mm]
4	42.38 [mm]	0.35 [mm]	1.00 [mm]
5	42.38 [mm]	0.35 [mm]	1.20 [mm]

Figure 4 shows the model profiles, detailing the backing and recovering thicknesses.

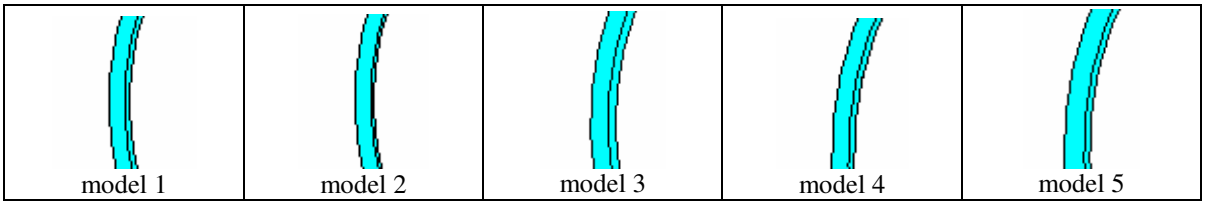

Figure 4. Each model profile (partial).

The bearing in study is a bearing with backing of steel (Modulus of Elasticity E of 207 [GPa] and Poisson coefficient ν of 0.292) and covering in babbitt (Modulus of Elasticity E of 50 [GPa] and Poisson coefficient ν of 0.33).

The bearing was considered fixed, that is, had been applied displacement restrictions in all direction. These restrictions had been applied externally to backing of the bearing, as it shows figure 5.

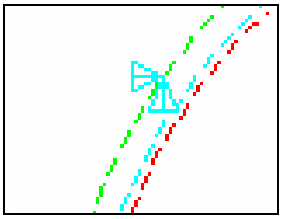

Figure 5. Detail of displacement constrain (triangles in the figure).

With the definition of the geometrical model it was proceeded the discrete finite elements model generation. For this, in all models, bidimensional, quadrilateral and isoparametric with eight nodes solid elements was used, that are called en the ANSYS environment for *PLANE 82*, which is shown in figure 6.

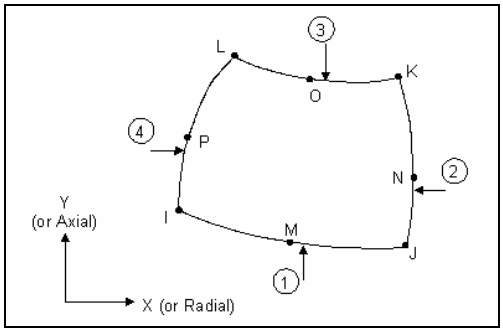

Figure 6. Scheme of the *PLANE 82* element.

For this analysis, a structuralized mesh was used, with solid element *PLANE* 82, witch possesses 8 nodes with 2 degree of freedom in each node. Table 3 shows the number of elements in the radial and circumferential directions, for each model.

Table 3. Number of elements in each model**.**

Model	Number of elements			
	Radial direction		Circumferential direction	
	Backing	Covering	Backing	Covering
1	6	4	150	150
2	6	3	150	150
3	6	4	150	150
4	5	4	150	150
5	7	4	150	150

4. Stress analysis in the models

First, real bearing (model 1) was simulated to obtain the active stresses, to can comparing with the gotten results of the other models. Figure 7a presents active circumferential stresses in the bearing. Although the circumferential stress is practically compression in the region where hydrodynamic pressure acts, in the end of this region, the circumferential stress become tensile. Figure 7b shows the shear stresses in the bearing.

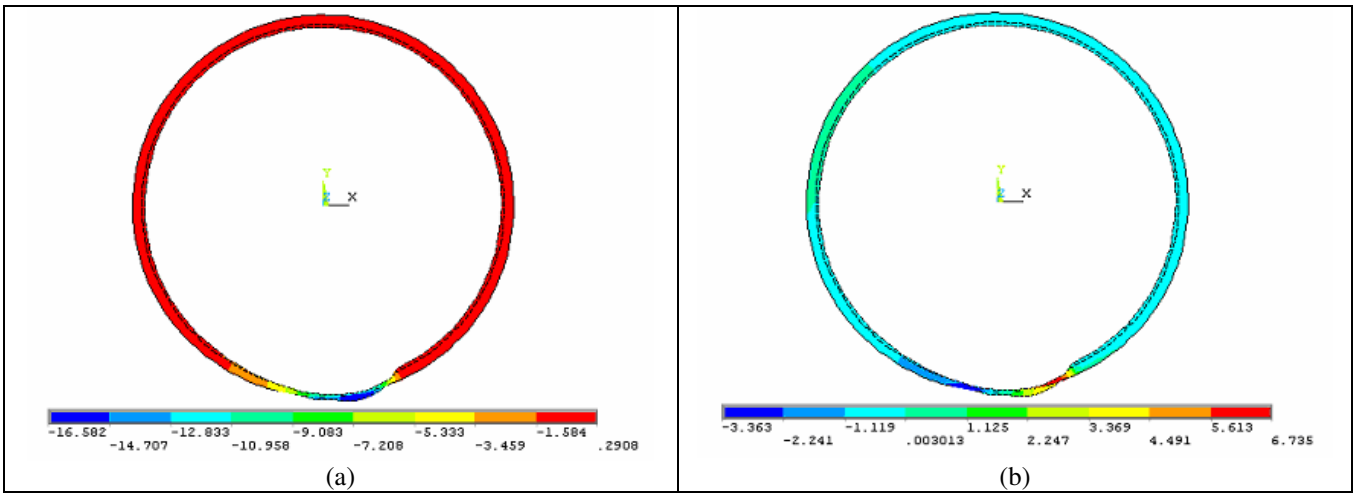

Figure 7. Circumferential stresses (a) and shear stresses (b) in the real model (model 1).

4.1. Variation in the covering thickness

In this stage two bearing models (models 2 and 3) was simulated differently of real model (table 2) with variation in the covering thickness (*babbitt*). Figure 8a shows the circumferential stresses for the model with covering thickness reduced (model 2). Figure 8b presents the shear stresses of the same model.

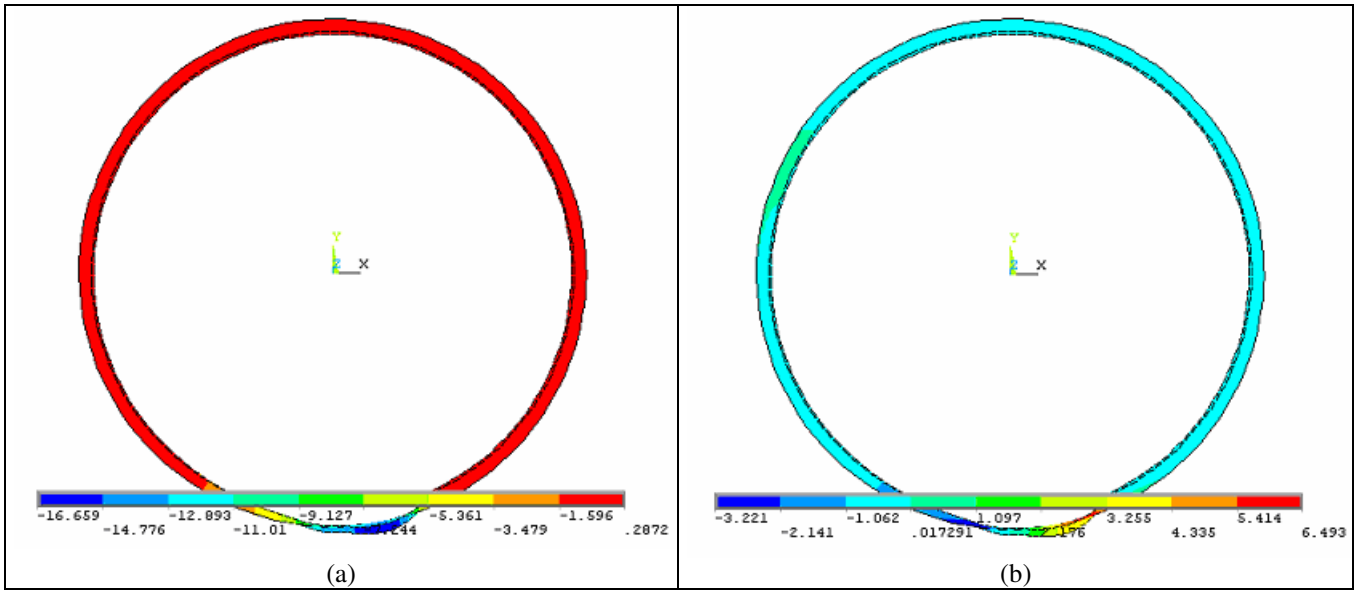

(a) (b)

Figure 8. Circumferential stresses (a) and shear stresses (b) in the model with the *babbitt* thickness reduced (model 2).

Figure 9a shows the circumferential stresses for the model with covering thickness increased (model 3). Figure 9b presents the shear stresses of the same model.

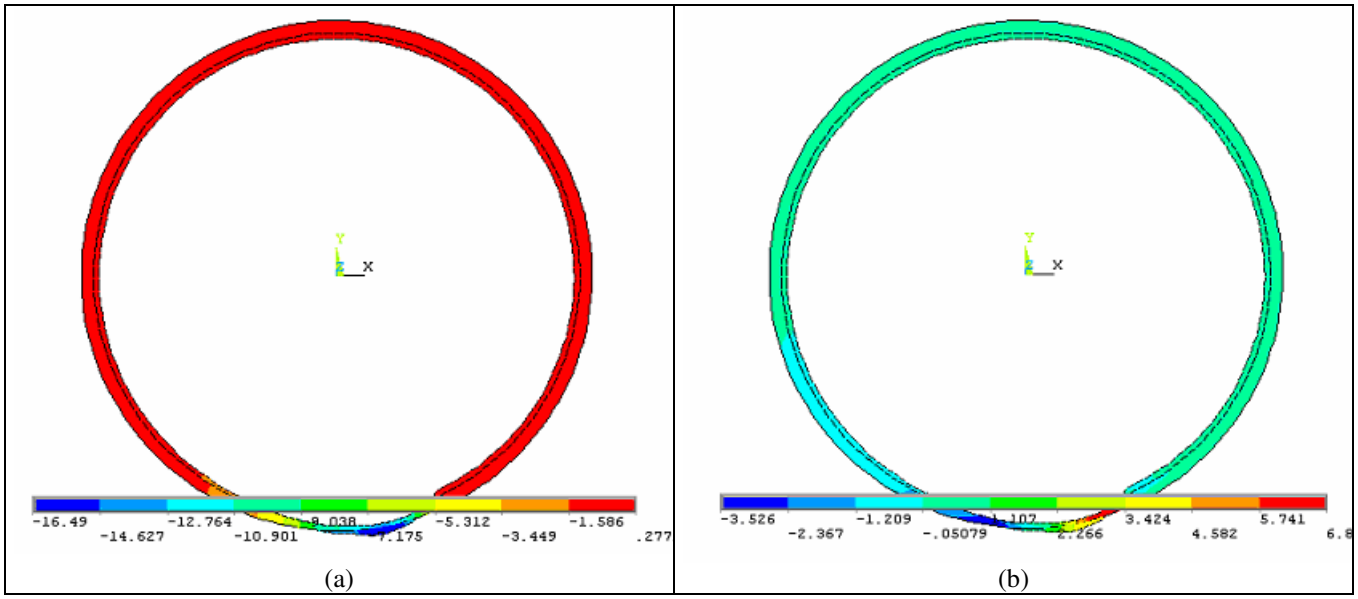

(a) (b)

Figure 9. Circumferential stresses (a) and shear stresses (b) in the model with the *babbitt* thickness increased (model 3).

It is verified that in the reduced covering thickness model (model 2) it has an improvement for shear stress, but the increased covering thickness model (model 3) has an improvement for circumferential stress.

4.2. Variation in the backing thickness

In this stage two different bearing models (models 4 and 5) was simulated with variation in the backing thickness. Figure 10a shows the circumferential stresses for the model with backing thickness reduced (model 4). Figure 10b presents the shear stresses of the same model.

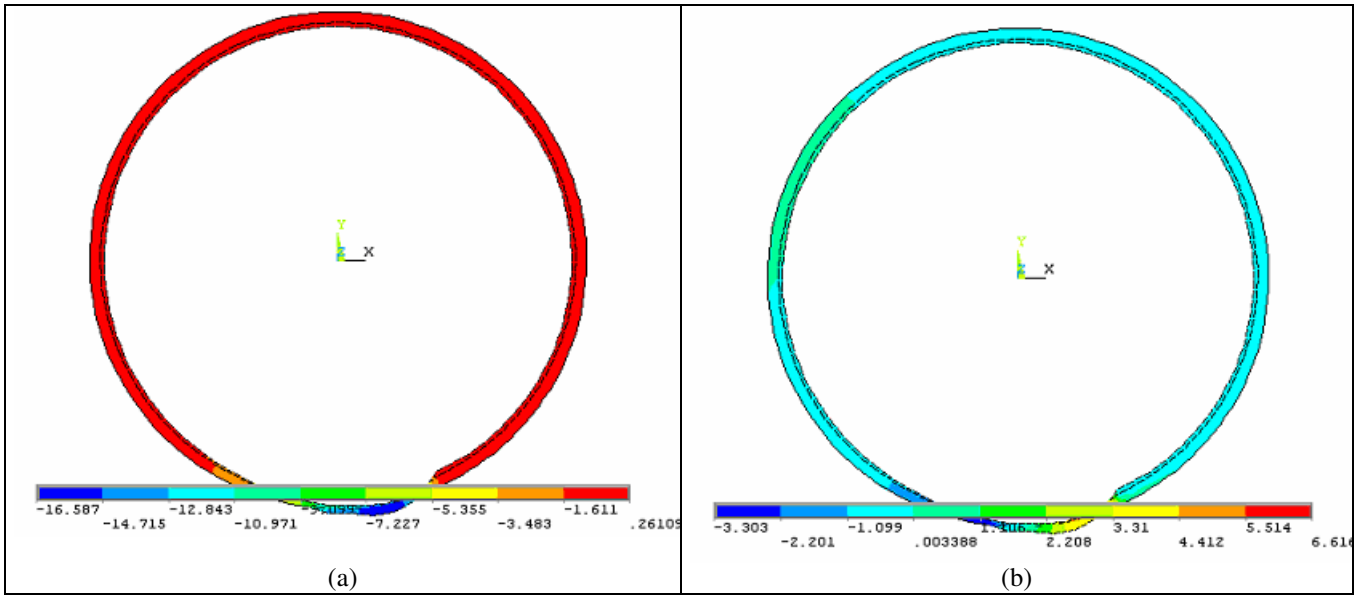

(a) (b)

Figure 10. Circumferential stresses (a) and shear stresses (b) in the model with the backing thickness reduced (model 4).

Figure 11a shows the circumferential stresses for the model with backing thickness increased (model 5). Figure 11b presents the shear stresses of the same model.

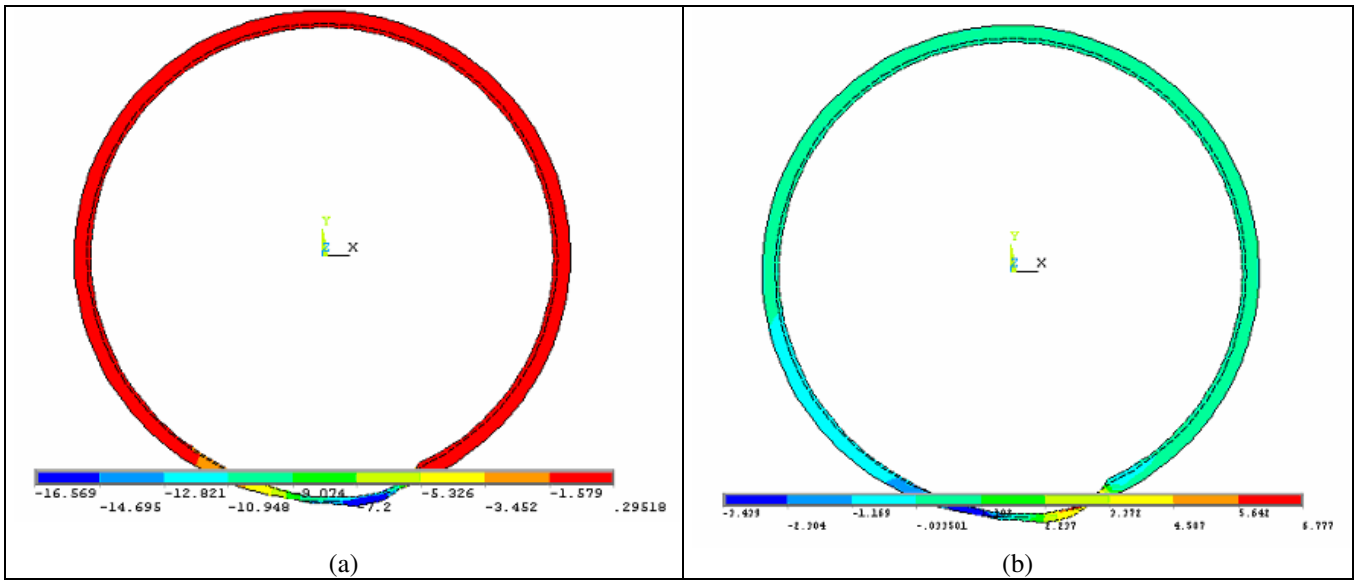

(a) (b)

Figure 11. Circumferential stresses (a) and shear stresses (b) in the model with the backing thickness increased (model 5).

4.3. Results and discussion

Table 4 shows the maximum values in module of the circumferential and shear stresses for each simulated model.

Table 4. Maximum circumferential and shear stresses for each model.

Stress Field	Model 1	Model 2	Model 3	Model 4	Model 5
Circumferential	16.582 [MPa]	16.659 [MPa]	16.490 [MPa]	16.587 [MPa]	16.569 [MPa]
Shear	6.735 [MPa]	6.493 [MPa]	6.899 [MPa]	6.616 [MPa]	6.777 [MPa]

With these results, if to compare the real model (model 1) with the other models is possible to note a small variation as much in the circumferential stress as in the shear stress. Another fact to be notice, is that the increase in the total bearing thickness, that is, an increase as much in the backing thickness as covering thickness, reduces the effective circumferential stress, but on the other hand, it increases the shear stress, that if to occur in the interface backing/covering it can generate fatigue failures. However, the reduction of total bearing thickness reduces the shear stress and increases the circumferential stress, what it can leave to fatigue failures in form of surface cracks.

5. Conclusions

With this simulation, it is possible to notice that the variation of the bearing thickness influences in the active stresses, as much in the circumferential stresses as in the shear stresses.

In the analyses of the circumferential and shear stresses, stress concentration regions are noticed. These stresses can favor the nucleation of fatigue cracks, because these appear mainly in the surface caused by high tensile stresses or in the interface between backing and covering caused by high shear stresses (Ibrahim e McCallion, 1970 and Blundell, 1979).

Therefore, it is important to define the backing and covering thicknesses in accordance with the stresses it desire to get and, also, to worry about the covering layer wear, what it can modify the bearing active stresses.

6. Acknowledgements

The present work was carried with the support of the "*Conselho Nacional de Desenvolvimento Científico e Tecnológico*" – CNPq – Brazil and "*Fundação de Amparo à Pesquisa do Estado de São Paulo*" – FAPESP – Brazil.

7. References

Blundell, J. K., *Fatigue Initiation in Thin-Wall Journal Bearings*, ASLE Transactions, vol. 33, 2, pp. 131-140, 1979.

Forrester, P. G., Chalmers, B., *Fatigue testing of bearing alloys*, Engineering, Vol. 159, 3p. , 1945.

Hacifazlioglu, S., Karadeniz, S., *A Parametric Study of Stress Sources in Journal Bearings*, Int. J. Mech. Sci., vol. 38, n. 8-9, pp. 1001-1015, 1996.

Ibrahim, S. M., McCallion, H., *Stresses in Oil Lubricated Bearings*, vol. 184, nº 3, pp. 69 – 78, Proc. Inst. Mech. Engrs., 1970.

Norton, R. L., *Machine Design: An Integrated Approach*, Prentice-Hall Inc., 1998.

8. Responsibility notice

The authors are the only responsible for the printed material included in this paper.